EARTH'S CRYOSPHERE
SCIENTIFIC JOURNAL

Earth`s Cryosphere, 2017, vol. XXI, No. 2, pp. 38–45 **http://earthcryosphere.ru/**

GAS HYDRATES FORMATION

DOI: 10.21782/EC2541-9994-2017-1(38-45)

NATURAL GAS HYDRATES FORMATION IN DISPERSED ICE STABILIZED WITH SILICA NANOPARTICLES

L.S. Podenko[1], A.O. Drachuk[2], N.S. Molokitina[1,2], A.N. Nesterov[1–3]

[1] *Earth Cryosphere Institute, SB RAS, 86, Malygina str., Tyumen, 625000, Russia; lpodenko@yandex.ru*
[2] *Tyumen State University, 6, Volodarskogo str., Tyumen, 625003, Russia*
[3] *Tyumen Industrial University, 38, Volodarskogo str., Tyumen, 625000, Russia*

The paper presents the study of natural gas hydrate formation in dispersed ice produced by either "dry water" freezing or by mechanical grinding with hydrophobic silica nanoparticles (stabilizer), along with the influence of the amount of stabilizer on dispersity of crushed ice and gas hydrate formation kinetics. It has been established that the time of half-transformation of dispersed ice into hydrate will decrease for frozen "dry water" with the increasing stabilizer content. For crushed ice, its half-transformation into hydrate will also take less time in case ice is ground with stabilizer, rather than without adding it. The time of half-transformation of dispersed ice into hydrate is found to be less than for frozen "dry water" with the stabilizer content of 5 wt.%, under identical conditions for water dispergating and ice grinding. If the content of stabilizer is 10 wt.%, the time of half-transformation of ice into hydrate will be less for frozen "dry water". The obtained results might be used in technologies related to transportation, storage, and utilization of natural gases in the hydrate state. Realization of these projects would be more effective under the low-temperature conditions of high latitude regions.

Gas hydrate, frozen "dry water", crushed ice, hydrophobic nanoparticles, nuclear magnetic resonance, hydrate formation kinetics

INTRODUCTION

Gas hydrates are crystalline compounds consisting of hydrogen-bonded water molecules configured into cage structures that enclose molecules of guest substances, and exist as gas under standard conditions for temperature and pressure (STP, 0 °C and 100 kPa). During dissociation of one volume of natural gas hydrate (NGH) at STP, up to 170 gas volumes are yielded, which makes applications of gas hydrates attractive to the actively developing alternative technologies for transportation, storage and utilization of natural and associated petroleum gases in the hydrate form [*Horiguchi et al., 2011; Rehder et al., 2012*].

Producing and storing gas hydrates requires relatively low temperatures and elevated pressure; further lowering the temperature allows to reduce the pressure required for gas hydrates formation. The gas hydrate technologies therefore appear to be the most promising primarily under conditions of low ambient temperatures, for example in the Arctic. The development of gas hydrate-based technologies in recent times is impeded by the lack of production technologies capable to maintain high (commercially viable) rates of hydrate formation.

One of the approaches to solving this problem is the application of dispersed ice to gas hydrates formation. The rate of hydrate formation can be enhanced at the expense of the increased ice–gas interface, and due to the fact that this ice–gas interface is more advantageous for hydrate formation, than the water–gas interface [*Melnikov et al., 2010*]. As is known, sintering of ice particles leads to a decrease in its dispersity [*Blackford, 2007*], lowering thereby the rate of hydrate formation. Dispersed ice persistent to sintering ("stabilized" ice) can be obtained by ice crushing with admixture of hydrophobic silica nanoparticles acting as a stabilizer [*Podenko and Molokitina, 2012; Melnikov et al., 2013*].

Alternatively, stabilization of dispersed ice can be achieved by the "dry water" freezing [*Podenko et al., 2015*]. "Dry water" is a free-flowing powder produced by high-speed mixing of ordinary water (up to 98 wt.%), hydrophobic silica nanoparticles and air [*Binks and Murakami, 2006*]. Water is contained in the powder as micron-sized individual drops or their aggregates [*Podenko et al., 2011*]. Adsorption of silica nanoparticles on the surface of micron-sized drops of water prevents their coalescence, insuring stability in such dispersed systems.

Recent research has shown that unlike bulk water, the application of "dry water" to gas hydrates

production process essentially enhances the rate of hydrate formation [*Wang et al., 2008; Carter et al., 2010; Ildyakov et al., 2011*]. This prompted to us an inference about "dry water" to serve a basis for viable system for gas hydrates production. Gas hydrate formation in the frozen "dry water" was analyzed in detail by L.S. Podenko and his colleagues [*Podenko et al., 2013*].

However, a possible influence of concentration of silica nanoparticles used for production of "dry water" and affecting the dispersion of ice formed during the freezing of "dry water" and therefore the rate of hydrate formation in dispersed ice, is still poorly understood. There is also a paucity of research on natural gas hydrates formation using crushed ice stabilized by hydrophobic nanoparticles. As such, the focus of our research has been narrowed to the latter topic.

PREPARATION OF "DRY WATER"

"Dry water" was produced by mixing distilled water and hydrophobic pyrogenic silica dioxide (here and further in the text, stabilizer) (total mixture weight: about 100 g) in a household blender Braun VX2050 at a speed of 18,700 rpm during 30 seconds. The stabilizer content in the mixture varied from 0.5 to 15 wt.%. In this research, we used Powders of nanoparticles of hydrophobic silica manufactured by Evonik Industries AG (Aerosil® R202 trademark) (here and further in the text, aerosil) or Wacker Chemical (HDK® H18) (here and further in the text, H18) as stabilizers.

The main parameters of the stabilizers used for producing dispersed ice by freezing "dry water" or by grinding ice are listed in Table 1 showing that carbon content and bulk density slightly differ for aerosil and H18 (whose specific surface area is much larger, though). However, the hydrate-forming abilities of "dry water" stabilized by Aerosil and H18 have not yet been compared.

"Dry water" is a polydisperse system. The analysis of size-distribution of aqueous droplets in "dry water" samples by visual methods appears to be time- and labor-taking. Therefore, we applied visual observations on optical microscope (Motic DM 111 Digital Microscopy) only for the purpose of qualitative analysis of dispersity of the investigated samples, whereas quantitative determinations of mean water-droplet sizes were carried out with the proton nuclear

Table 1. **Main parameters of silica dioxide nanoparticles [*HDK® H18..., 2016; Hydrophobic..., 2016*]**

Paramerter	Silica dioxide	
	H18	Aerosil
Carbon content, %	4.6	4.3
Bulk density, g/L	50	60
Specific surface, m^2/g	200	100

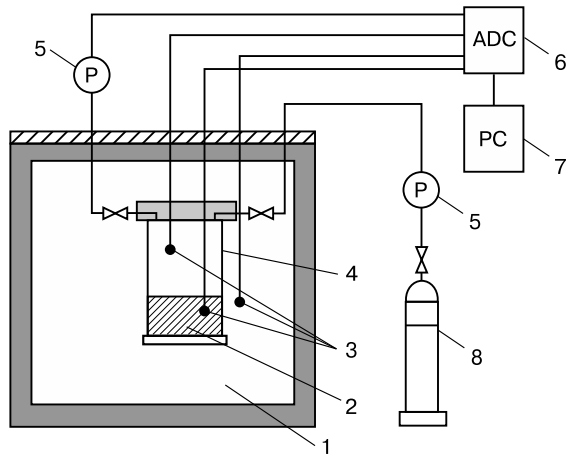

Fig. 1. Schematics of the experimental apparatus:

1 – thermostat; 2 – sample; 3 – thermal gauges; 4 – reactor; 5 – manometer; 6 – analogue-to-digital converter; 7 – computer; 8 – gas bulb.

magnetic resonance (NMR) [*Melnikov et al., 2011; Podenko et al., 2011*].

Nuclear-magnetic relaxation was measured with a Bruker Minispec mq pulsed NMR relaxometer (resonance frequency: 20 MHz). In the experiment, the well known Carr–Parsell–Meibum–Gill (CPMG) technique was realized to determine the spin-spin relaxation time T_2 [*Slichter, 1990*]. The nuclear magnetization decay curves were processed with approximations of data by one- and two-exponential curves, and supplemented by an inverse Laplace transformation of the signal decay function of relaxation for calculating time or spectrum (frequency distribution) of relaxation times for nuclear magnetization [*Provencher, 1982*]. The resultant data were used to determine mean size of water droplets in the "dry water" samples following the procedure reported in [*Podenko et al., 2011*].

PREPARATION OF DISPERSED ICE

The two modes used to produce dispersed ice were: 1) freezing of "dry water"; 2) mechanical grinding during 30 seconds of ordinary ice, adding powdered stabilizer nanoparticles into the grinding chamber. For the "dry water" freezing, its sample weighing 7 g at room temperature was placed into a temperature-controlled high-pressure reactor, which can also be used to produce gas hydrates (Fig. 1). The reactor was then cooled down to –20 °C at a constant rate of 2 °C/min.

The exothermic peak was observed in the temperature interval between –6 and –10 °C, on the thermogram obtained from the cooled sample, indicating the freezing of water droplets. The crystallization of water was completed at a temperature of about –10 °C. After cooling to –20 °C, the frozen sample of

"dry water" was removed from the reactor for further analysis of its properties.

The ice was mechanically ground in a Teledoor thermostated chamber at –20 °C on the aforementioned equipment and the applied speed was equal to that used for the preparation of "dry water" (Braun VX2050 blender, 18,700 rpm).

The dispersion composition of the prepared frozen "dry water" and ground ice samples was determined by the sieve analysis using laboratory screens with calibrated 1000, 700, 500, 400, 200, 160, 140 and 80-micron openings. The samples were sieved on PE-6700 electro-dynamical shaker with 20 Hz frequency of the worktable vibration at the ambient temperature –20 °C.

GAS HYDRATES PREPARATION

Schematics of the experimental apparatus for gas hydrate preparation is shown in Fig. 1. Natural gas sampled from the Urengoy–Surgut–Chelyabinsk gas pipeline was used as the hydrate-forming gas (mol.%): C_1H_4 – 98.6, C_2H_6 – 0.46, C_3H_8 – 0.24, C_4H_{10} – 0.06, C_5H_{12} – 0.02, CO_2 – 0.15, N_2 – 1.01. Hydrate was form in a stainless steel high-pressure reactor with a volume of 60 cm^3.

For hydrate synthesis, equal amount of about 7 g of either "dry water" or crushed ice, was loaded into the reactor. The "dry water" was loaded at room temperature, while loading the ground ice into the reactor proceeded in the Teledoor refrigerator chamber at –20 °C. After that, natural gas was slowly blown through the reactor at atmospheric pressure, to remove the air. The reactor was placed in a thermostat and cooled down to –20 °C to freeze the "dry water". The freezing of sample was monitored through the control of its cooling thermograms. This step was followed by the reactor warming up to –1 °C and its filling with natural gas until pressure reached 4.6 MPa. The same procedure was done for the ground ice once it was loaded in the reactor at –20 °C. The rate of gas hydrates formation from ice is known to be increasing sharply as the hydrate formation temperature increases to the melting point of ice [*Hwang et al., 1990; Staykova et al., 2003*]. This was why we opted for –1 °C as the temperature for the hydrate formation (close to the melting temperature of ice, taking into account the correction for the pressure in the reactor).

Hydrate formation took place under isochoric conditions during 80 h and occurred with a decrease of the pressure in the reactor. The amount of moles Δn of gas uptake during the hydrate formation was calculated by the equation

$$\Delta n = pV/(ZRT)_0 - pV/(ZRT)_t, \qquad (1)$$

where V is gas volume in the reactor; R is the universal gas constant; p, T are pressure and temperature in the reactor; Z is the compressibility factor calculated using the Peng-Robinson equation of state. Indices 0 and t are the initial (immediately after filling the reactor with gas) and the current time, respectively.

RESULTS AND DISCUSSIONS

"Dry water" samples were obtained by the authors using a stabilizer in the amount of 0.5, 1.0, 1.5, 2.0, 3.0, 5.0, 10 and 15 wt.%. In case the stabilizer content was less than 2 wt.%, the resulting sample became quickly (a matter of few minutes) stratified into bulk liquid water and stabilizer powder with inclusions of water droplets (Fig. 2). Given a higher content of the stabilizer, we obtained a stable (within the time frame of the experiment) "dry water" dispersion.

According to the data of visual observations (Fig. 3) and NMR measurements (Table 2), an increase in the stabilizer (both aerosil and H18) content resulted in a decrease in the size of microdroplets of water in the "dry water" samples. Given the same content of aerosil and H18, droplets in "dry water" stabilized by H18 had a smaller average size than in

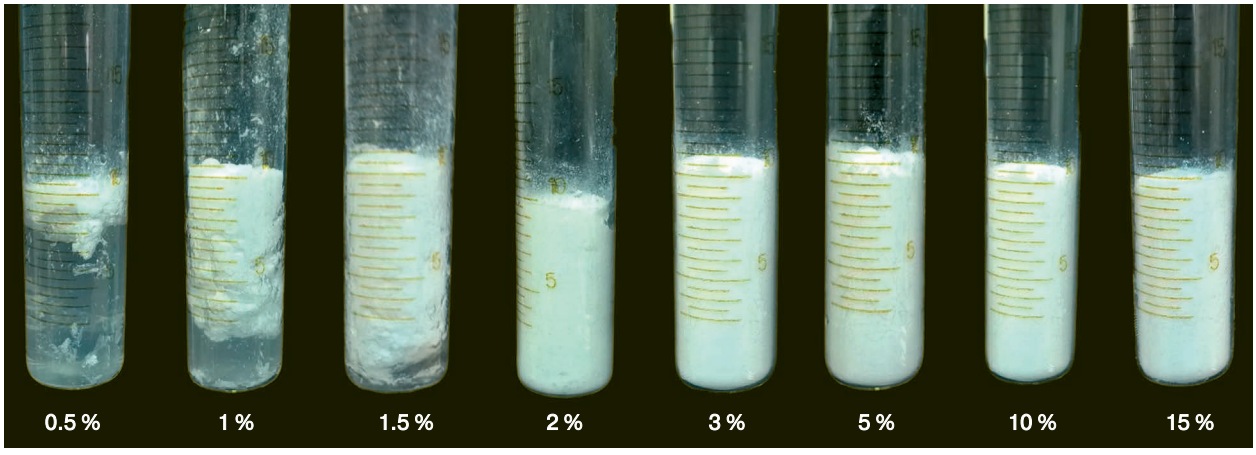

Fig. 2. Samples of "dry water" with aerosil content from 0.5 to 15 wt.%.

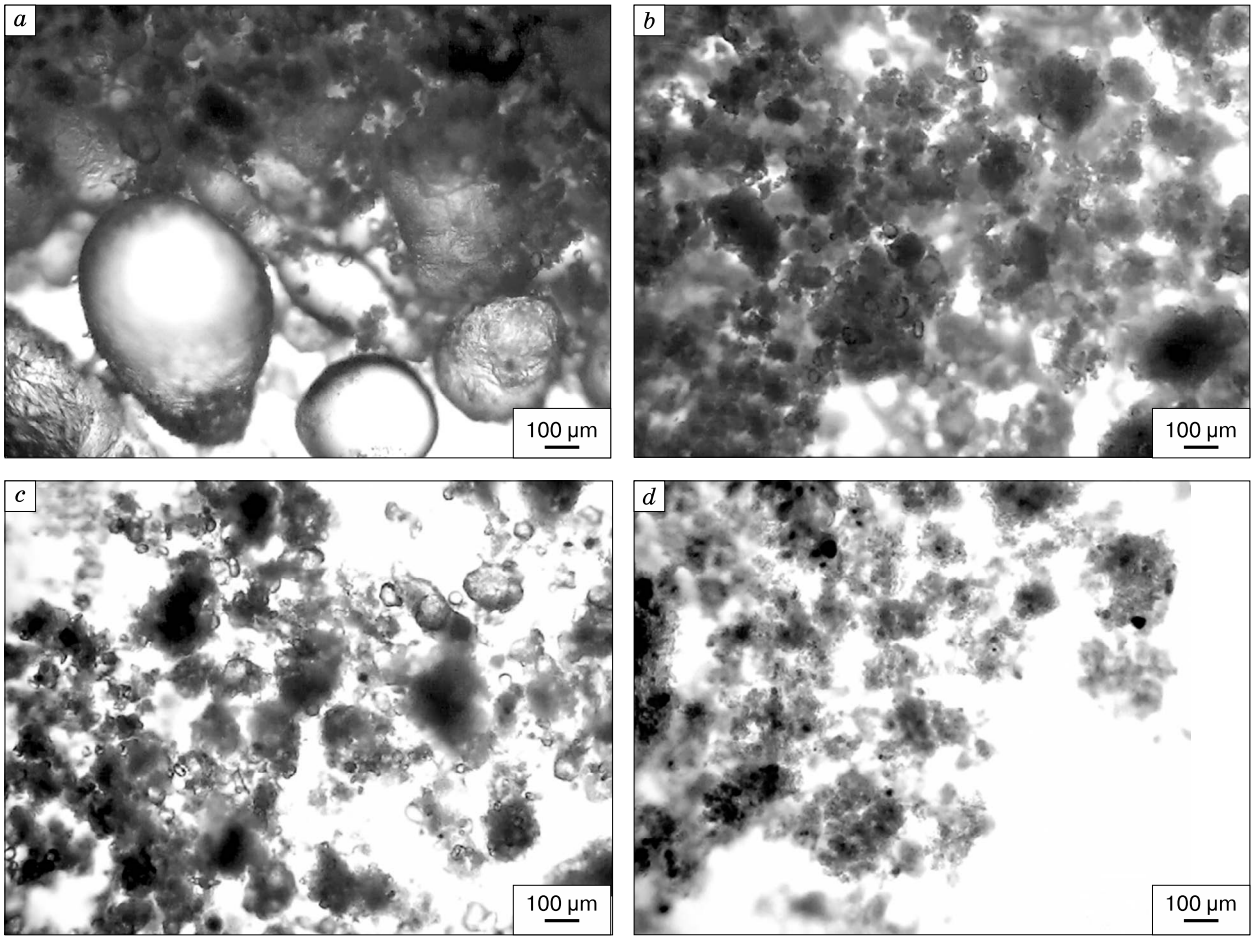

Fig. 3. Microphotographs of "dry water" with H18 contents:
a – 3 wt.%; *b* – 5 wt.%; *c* – 10 wt.%; *d* – 15 wt.%.

the "dry water" stabilized by aerosil (Table 2). The latter is probably is accounted for by the specific surface area value being 2 times greater for H18 than for aerosil (Table 1).

Fig. 4 illustrates two samples of the frozen "dry water" with a stabilizer content of 5 and 10 wt.% after they are removed from the reactor (at –20 °C). It has been found that frozen "dry water" with the stabilizer content not more than 5 wt.% represents by itself solid, frozen mass slightly admixed with bulk material in the form of white powder (Fig. 4, *a*) consisting mainly of ice particles. If the stabilizer content in the "dry water" is above 5 wt.%, the proportion of the powder in the sample increases (Fig. 4, *b*). As shown by the fractional composition analysis carried out at $T = -20$ °C, the powder was completely sieved through a screen with a mesh size of 700 μm. The weight content of the powder fraction with a particle size of 0–700 μm was determined from the frozen "dry water" sample (Table 3). As can be deduced from the data listed in Table 3 it has grown from 0.06 to 1.0 wt.% in parallel with the stabilizer content in the "dry water" (from 3 to 15 wt.%). This suggests that an increase in the stabilizer content in the "dry water" has caused a greater dispersity of ice produced from its freezing.

The sieve analysis data allowed to determine a dispersed composition of the crushed ice, with the average particle size distribution of ice calculated based on the known technique by [*Kouzov, 1987*].

Table 2. **Mean particle size of water droplets in the "dry water" samples from NMR data**

Stabilizer	Stabilizer concentration, wt.%	Mean particle size of water droplets, μm
Aerosil	3	13
	5	10
	10	8
	15	6
H18	5	8
	10	5

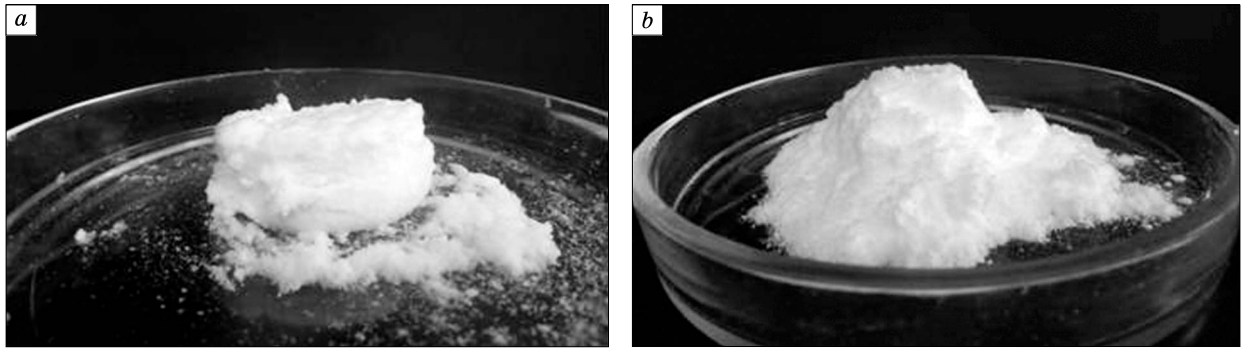

Fig. 4. Samples of frozen "dry water" after retrieval from the reactor.
H18 contents in the samples: *a* – 5 wt.%; *b* – 10 wt.%.

Table 3. **Mass ratio of the particle fraction with a size of 0–700 μm in "frozen water" samples**

Aerosil contents in the "dry water" sample, wt.%	Mass ratio of the 0–700 μm fraction, rel. un.
3	0.06
5	0.20
10	0.94
15	1.00

The results obtained are shown in Fig. 5 and in Table 4. As follows from the latter, the additional input of hydrophobic silica nanoparticles provoked a more than 2-fold decrease in the average grain size of crushed ice compared to ice ground without such additive. At this, an increase (from 5 to 10 wt.%) in the content of an additive slightly affected the variation in the crushed ice dispersity, which was not the case with the samples of frozen "dry water" where in response to the increased concentration of the stabilizer (from 5 to 10 wt.%) the fraction of particles have shown almost 5-fold increase (Table 3). We also note

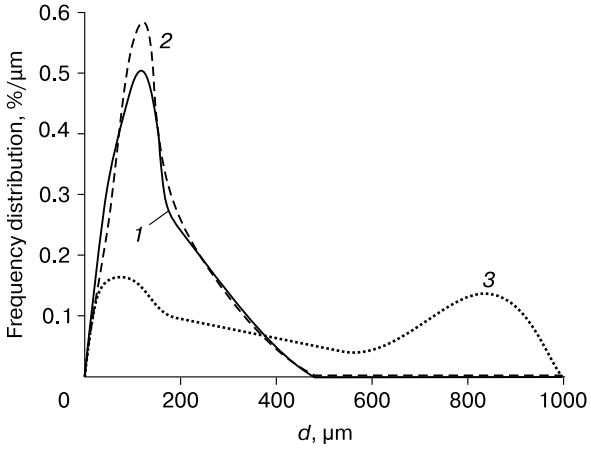

Fig. 5. Particle size distribution of the ice crushed with admixture of aerosil in the amount of 5 wt.% (*1*), 10 wt.% (*2*) and without this additive (*3*).

that the average grain size of crushed ice obtained by grinding with admixture of aerosil and using H18 remained practically unchanged.

The formation of natural gas hydrates was studied by the authors under isochoric conditions at a temperature of $T = -1$ °C and initial pressure $p_0 = 4.6$ MPa for samples of frozen "dry water" and ground ice with stabilizer content of 3, 5, 10 and 15 wt.%. For comparison, control experiments were conducted with crushed ice (with an average particle size of 500 μm) obtained without the stabilizing additive.

In both the cases of hydrate formation from the frozen "dry water" and crushed ice stabilized with hydrophobic silica nanoparticles, as well as in the control experiment with crushed ice prepared without adding any stabilizer, there was observed a pressure reduction in the reactor, once its filling with gas was completed, which is associated with the hydrate formation and is indicative of its proceeding without an induction or lag period.

Using data on the amount of natural gas uptake during the hydrate formation (equation (1)), it is possible to calculate the amount of hydrate formed. To this end, the composition of the hydrates formed should be known. A gas hydrate composition is determined by the stoichiometric ratio $G{\cdot}nH_2O$, where G is the gas-hydrate-forming component; n is the hydrate number (the number of water molecules per one molecule of gas hydrate-former in hydrate). Natural gas containing 0.2 mol.% of propane forms mixed hydrates with CS-II structure [*Istomin and Yakushev,*

Table 4. **Mean particle size of the crushed ice, ground with and without additive**

Stabilizer	Content, wt.%	Mean particle size, μm
no	0	500
Aerosil	5	175
Aerosil	10	165
H18	5	160

1992], which have n = 5.66 if all cavities are filled with gas molecules. Gas hydrates being non-stoichiometric clathrate compounds, however, their degree of cavity occupancy is less than 1 and is controlled by the hydrate formation conditions (i.e. in our case, n will be greater than 5.66). In addition, n is largely influenced by the composition of natural gas. The CSMGem software [*Sloan and Koh, 2008*] enabled us to calculate n on the water (ice)–hydrate–gas equilibrium line. The calculations showed that for a temperature value of –1 °C, the equilibrium hydrate formation pressure for the natural gas used in our work is 1.67 MPa, and n = 6.58.

The calculation accuracy for n can be estimated by comparing its results with the known experimental data, for example, for methane hydrate. The average value of n for methane hydrate on the water (ice)–hydrate–gas equilibrium line according to the experimental data obtained by C. Circone with collaborators [*Circone et al., 2005*] equals 6.0 and does not change with the increasing pressure along the equilibrium curve in the temperature range from –10 to +12 °C, whereas the calculations showed that n = 6.27 at the equilibrium pressure and T = –10 °C, and n = 6.04 at the water–hydrate–gas equilibrium at +12 °C. According to the calculations, at the equilibrium pressure 2.47 MPa and a temperature –1 °C, n = 6.31 for methane hydrates, which is about 5 % higher than the experimental values. An increase in pressure at a given temperature versus the equilibrium pressure of hydrate formation also causes a decrease in n. Thus, for methane hydrate, a 2-fold increase in the hydrate formation pressure versus the equilibrium pressure, leads to a decrease in the hydrate number by about 5 % (from 6.1 to 5.8) [*Circone et al., 2005*].

We note that the equilibrium pressure of natural gas hydrates formation in our experiments at –1 °C (1.67 MPa) is almost 3 times less than the initial pressure of the gas charged to the reactor (4.6 MPa). Although the pressure in the reactor was constantly decreasing during the isochoric formation of natural gas hydrates, by the time the hydrate formation had ceased, it remained measurably higher (2.8 MPa) than the equilibrium pressure. With consideration of the above discussed, we assume that n = 6.0 for natural gas hydrates, which is approximately 10 % less than the calculated value (n = 6.58). Also, it should be borne in mind that the hydrates formed under isochoric conditions with an excessive amount of natural gas (as in our experiments) represent a mixture of methane hydrates (CS-I structure, n = 6.0) and mixed natural gas hydrate (CS-II) [*Uchida et al., 2004; Nesterov, 2006; Medvedev et al., 2015*].

Hence, in our calculations the amount of formed hydrate was derived from the hydrate composition determined by the $G{\cdot}6H_2O$ ratio. Then the ice-to-hydrate conversion degree Δh (mass of ice transferred into hydrate divided by the initial ice mass in the sample) is calculated as follows:

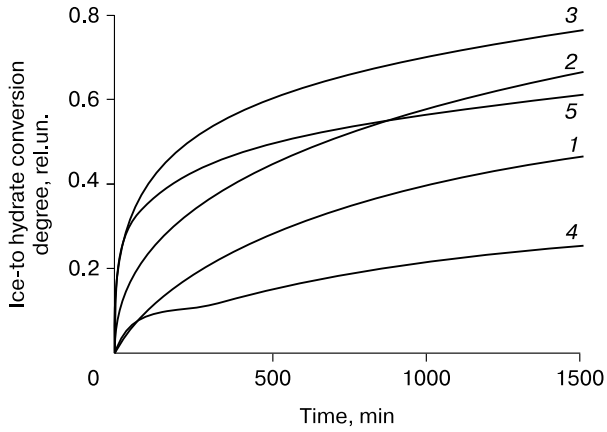

Fig. 6. Changes in the dispersed ice-to-natural gas hydrate conversion degree (T = –1 °C, p_0 = 4.6 MPa) **for frozen "dry water" (*1–3*) and for ice ground without adding the stabilizer (*4*) and with adding H18** (5 wt.%) **(*5*).**

H18 content in the "dry water": *1* – 5 wt.%; *2* – 10 wt.%; *3* – 15 wt.%.

$$\Delta h = (6M_w\Delta n)/m,$$

where M_w is molar mass of water; m – initial ice-mass in the analyzed sample.

Fig. 6 shows a characteristic behavior of the kinetic curves illustrating the transformation of dispersed ice into natural gas hydrate for the samples of frozen "dry water" and crushed ice. It follows from these data that the rate of hydrate formation, definedas $\Delta h/\Delta t$, is a variable value, strongly slowing down with time. Therefore, the half-reaction time of ice-to-hydrate conversion ($t_{1/2}$), i.e, the time during which Δh reached the value of 0.5, was assumed to be the average kinetic characteristic of the gas hydrates formation.

The inverse of the half-reaction time ($1/t_{1/2}$), can be considered as the average rate of ice-to-hydrate conversion at a given time interval. The smaller the value of $1/t_{1/2}$, the greater is the average rate of hydrate formation. The results of the calculations are given in Table 5. As follows from Table 5, with the increasing content of silica dioxide in the samples of frozen "dry water" from 3–5 to 15 wt.%, the $t_{1/2}$ time has decreased by more than 7–15 times, depending on which of the stabilizers (aerosil or H18) was used to prepare "dry water". We relate this result to the increased dispersity of ice in the frozen "dry water" with an increase in the silica dioxide content (Table 3).

A relation between the half-reaction time of dispersed ice converting into a hydrate and the ice particles size distribution was also observed in the crushed ice. The use of an additive for the ice grin-

Table 5. **Half-reaction time of ice-to-hydrate conversion during hydrate formation at isochoric conditions in the samples of "dry water" and crushed ice**

Stabilizer	Stabilizer content, wt.%	Half-reaction time, min
Frozen "dry water"		
Aerosil	3	2750
Aerosil	5	3350
Aerosil	10	1020
Aerosil	15	150
H18	5	1750
H18	10	650
H18	15	240
Crushed ice		
–	0	4800
Aerosil	5	1700
Aerosil	10	1500
H18	5	510

Note. Temperature $T = -1$ °C, initial pressure $p_0 = 4.6$ MPa.

ding allows to reduce grain size of the crushed ice (Table 4). This is, in our opinion, what accounts for a decrease in $t_{1/2}$ time for the dispersed ice obtained with adding the stabilizer, versuc ice ground without it (Table 5). Besides, a significant effect (almost a 10-fold reduction of $t_{1/2}$) is achieved, once the stabilizer is added in the amount of 5 wt.%.

We analyzed the impact of the technique for obtaining dispersed ice (freezing of "dry water" or mechanical crushing of ice) on the ice particle size distribution and the kinetics of its transformation into a hydrate. According to the data listed in Table 4, the average particle size of the crushed ice obtained by grinding with added 5 wt.% aerosil was 175 μm, while the frozen "dry water" with the same content of aerosil for the most part represented by itself a frozen ice mass (Table 3). As a result, the half-time of ice-to-hydrate conversion was several times less in the ground ice than in the frozen "dry water" containing 5 % by weight of the stabilizer. An increase in the aerosil concentration in "dry water" to 10 wt.% has led to an increase in the dispersity of frozen "dry water" (mass content of the free-flowing fraction became almost 5 times larger, compared to the frozen "dry water" containing 5 wt.% of the stabilizer, Table 3). At the same time, the average particle size distribution of the crushed ice changed insignificantly when the aerosil concentration increased to 10 wt.% (Table 4). As a result, with a stabilizer concentration being 10 wt.% in the sample, the $t_{1/2}$ time for the frozen "dry water" was less than for crushed ice.

When estimating the influence of the stabilizer type (aerosil and H18) on the half-reaction time of dispersed ice-to-hydrate conversion, we inferred from the analysis data that $t_{1/2}$ is significantly lower in the frozen "dry water" and in ice crushed using H18, as against the stabilized aerosil (Table 5). This probably is associated with a greater H18 specific surface area in comparison with aerosil, however the nature of this relation has not been fully understood by the authors.

CONCLUSIONS

It has been found that the frozen "dry water" containing not more than 5 wt.% of silica is a solid, frozen mass with a small admixture of free-flowing material in the form of white powder consisting mainly of ice particles. Once the silica concentration exceeds 5 wt.%, the free-flowing fraction in the sample of the frozen "dry water" will grow, approaching 1 at 15 wt.% concentration of silica nanoparticles.

It is shown that the half-reaction time of ice-to-hydrate conversion decreased with the increasing content of silica dioxide nanoparticles. Given the latter thus increases from 3–5 to 15 wt.%, the half-conversion time becomes more than 7–15 times greater, depending on the type of silica used to prepare the "dry water".

It has been established that for the crushed ice prepared by grinding of ordinary ice admixed with silica nanoparticles, the half-reaction time of ice-to-natural gas hydrate conversion is reduced by an order compared with the ice crushed without such additive. It is shown that under identical conditions for water dispersion and ice crushing, the half-reaction time is several times lower for the crushed ice than for the frozen "dry water" containing 5 wt.% of stabilizer nanoparticles in the test samples. With the stabilizer content being 10 wt.%, the half-reaction time will be less in the frozen "dry water".

The type of stabilizer used for grinding the ice is found to affect the rate of hydrate formation in the crushed ice. Thus, the half-reaction time for the crushed ice stabilized with H18 (specific surface area: 200 m^2/g) was 3 times less than for the crushed ice stabilized with aerosil (specific surface area: 100 m^2/g), with the same stabilizer content (5 wt.%).

The research results obtained can be translated into specific practical applications for developing technologies related to transportation, storage and utilization of natural gases in the form of hydrates. Their realization would be most effective in northern latitudes regions with their severe ambient low- temperature conditions.

The work was supported by the Russian Foundation for Basic Research (project No. 16-38-00279), the Council for Grants of the President of the Russian Federation for the state support of young Russian scientists (MK-8546.2016.8) and the state support for leading scientific schools of the Russian Federation (NSh-9880.2016.5), and by the RAS Presidium (the Fundamental Research Program "Fundamental scien-

tific research for benefits of development of the Arctic regions of the Russian Federation").

References

Binks, B.P., Murakami, R., 2006. Phase inversion of particle-stabilized materials from foams to dry water. Nature Materials, 5, 865–869.

Blackford, J.R., 2007.Sintering and microstructure of ice: a review. J. Physics D: Appl. Phys. 40 (21), p. R355–R385.

Carter, B.O., Wang, W., Adams, D.J., et al., 2010. Gas storage in "dry water" and "dry gel" clathrates. Langmuir, 26, 3186–3193.

Circone, S., Kirby, S., Stern, L., 2005. Direct measurement of methane hydrate composition along the hydrate equilibrium boundary. J. Phys. Chemistry B, 109, 9468–9475.

HDK® H18 Wacker Chemie AG. – URL: http://www.wacker.com/cms/en/products/product/product.jsp?product=9322 (submittal date: 28.01.2016).

Horiguchi, K., Watanabe, S., Moriya, H., et al., 2011. Completion of natural gas hydrate (NGH) overland transportation demonstration project, in: Proc. of the 7th Intern. Conf. on Gas Hydrates (Edinburgh, Scotland, UK). Paper No. P5.053.

Hwang, M.J., Wright, D.A., Kapur, A., Holder, G.D., 1990. An experimental study of crystallization and crystal growth of methane hydrates from melting ice. J. Inclusion Phenomena and Molecular Recognition in Chemistry, 8, 103–116.

Hydrophobic fumed silica – AEROSIL® fumed silica. – URL: http://www.aerosil.com/product/aerosil/en/products/hydrophobic-fumed-silica/pages/default.aspx (submittal date: 28.01.2016).

Ildyakov, A.V., Larioniov, E.G., Manakov, A.Yu., Fomin, V.M., 2011. Gas hydrate method with the use of "dry water" for natural gas enrichment with helium. Gazokhimia, No. 1, 28–32.

Istomin, V.A., Yakushev, V.S., 1992. Gas Hydrates at Natural Conditions. Nedra, Moscow, 237 pp. (in Russian)

Kouzov, P.A., 1987. Fundamentals of the Analysis of Dispersed Composition of Industrial Dusts. Khimia, Leningrad, 264 pp. (in Russian)

Medvedev, V.I., Gushchin, P.A., Yakushev, V.S., Semenov, A.P., 2015. Study of the effect of the degree of overcooling during the formation of hydrates of a methane-propane gas mixture on the equilibrium conditions of their decomposition. Chemistry and technology of fuels and oils, No. 5, 470–479.

Melnikov, V.P., Nesterov, A.N., Reshetnikov, A.M., et al., 2010. Stability at growth of gas hydrate below the ice-hydrate-gas equilibrium line on the *P–T* phase diagram. Chem. Eng. Science, 65, 906–914.

Melnikov, V.P., Podenko, L.S., Nesterov, A.N., Komisarova, N.S., Shalamov, V.V., Reshetnikov, A.M., Larioniov, E.G., 2011. Freezing of water drops in the dispersion of "dry water". Kriosfera Zemli, XV (2), 21–28.

Melnikov, V.P., Podenko, L.S., Nesterov, A.N., at al., 2013. Method for ice dispergation: Patent 2473850 Rus. Federation: MPK: F25C 5/02, B02C 19/00 / Claimant and patent owner: IKZ SO RAN (Institute of the Earth Cryosphere SB RAS). № 2011125973/13. Application date: 23.06.2011. Published: 27.01.2013. Bull. # 3.

Nesterov, A.N., 2006. Kinetics and mechanisms of gas hydrate formation in the presence of surface-active compound: Dissert. ...Dr. Sci. in chem., Tyumen, 280 pp. (in Russian)

Podenko, L.S., Molokitina, N.S., 2012. Solid micro-particles effect on ice crushing, in: Proc. of the 10th International Conference on Permafrost "Resources and Risks of Permafrost Areas in a Changing World" (Salekhard, June 25–29 2012). Salekhard, Pechatnik, pp. 423–426.

Podenko, L.S., Melnikov, V.P., Nesterov, A.N., et al., 2015. Building of ice dispersion system stabilized by hydrophobic fumed silica nanoparticles as new material for natural gas hydrate storage, in: Proc. of the Intern. Conf. on Material Science and Application ICMSA 2015 (Suzhou, China), pp. 300–304.

Podenko, L.S., Nesterov, A.N., Drachuk, A.O., et al., 2013. Formation of propane hydrates in frozed dry water. Russian J. Appl. Chemistry, 86 (10), 1509–1514.

Podenko, L.S., Nesterov, A.N., Komisarova, N.S., et al., 2011. Proton magnetic relaxation in a disperse "dry water" nanosystem. J. Appl. Spectroscopy, 78 (2), 260–265.

Provencher, S.W., 1982. A constrained regularization method for inverting data represented by linear algebraic equations. Computer Phys. Communications, 27, 229–242.

Rehder, G., Eckl, R., Elfgen M., et al., 2012. Methane hydrate pellet transport using the self-preservation effect: A techno-economic analysis. Energies, 5 (7), 2499–2523.

Slichter, C.P., 1990. Principles of Magnetic Resonance (3rd ed.). Series: Springer Series in Solid-State Sciences. Heidelberg, Springer, vol. 1, 657 pp.

Sloan, E.D., Koh, C.A., 2008. Clathrate Hydrates of Natural Gases, 3rd ed. CRC Press, New York, 721 pp.

Staykova, D.K., Kuhs, W.F., Salamatin, A.N., Hansen, T.J., 2003. Formation of porous gas hydrates from ice powders: diffraction experiments and multistage model. J. Phys. Chemistry B, 107 (37), 10299–10311.

Uchida, T., Moriwaki, M., Takeya, S., et al., 2004. Two-step formation of methane–propane mixed gas hydrates in a batch-type reactor. AIChE J., 50, 518–523.

Wang, W., Bray, C.L., Adams, D.J., et al., 2008. Methane storage in dry water gas hydrates. J. Amer. Chem. Society, 130 (35), 11608–11609.

Received March 1, 2016